



A Two-stage Micro Resistive Pulse Immunosensor for Pathogen Detection

Journal:	<i>Lab on a Chip</i>
Manuscript ID	LC-ART-10-2015-001207.R1
Article Type:	Paper
Date Submitted by the Author:	22-Dec-2015
Complete List of Authors:	Han, Yu; University of Akron, Mechanical Engineering Department Wu, Haiyan; University of Akron, Department of Chemical and Biomolecular Engineering Cheng, Gang; University of Akron, Department of Chemical and Biomolecular Engineering Zhe, Jiang; The University of Akron, Mechanical Engineering Department

ARTICLE

A Two-stage Micro Resistive Pulse Immunosensor for Pathogen Detection

Cite this: DOI: 10.1039/x0xx00000x

Yu Han,^{‡a} Haiyan Wu,^{‡b} Gang Cheng^{*b} and Jiang Zhe^{*a}

Received 00th January 2012,

Accepted 00th January 2012

DOI: 10.1039/x0xx00000x

www.rsc.org/

We present a two-stage immunosensor for pathogen detection in a mixed population. In this approach, antibody-conjugated microparticles were used to functionalize the surface of the capture chamber via a convenient magnetic method and a two-stage resistive pulse sensor was used to detect and quantify pathogen cells. We firstly tested the capture efficiency of the functionalized capture chamber. The specific capture efficiency of *S. cerevisiae* is greater than 94.8%, while the non-specific capture efficiency is 3.4%. We showed the device can accurately measure pure *S. cerevisiae* at concentrations ranging from 1.0 to 8.0×10^3 cells/ μL . We performed *S. cerevisiae* measurements in a mixture with *Chlorella*. Both cells have similar sizes. For *S. cerevisiae* to *Chlorella* ratio ranging from 1.0 to 2.0, the measurement errors was less than 7%, while the error became 20% to 32% for lower ratios ranging from 0.1 to 0.5 caused by nonspecific attachment. We demonstrated that this device is able to isolate target cell and quantitatively measure the cell population in a short time. This device can be potentially used for pathogen detection in food industry, biological research and clinical applications.

Introduction

Pathogen detection represents an important task for many applications such as disease diagnosis, food industry, environmental monitoring, biodefense and biological research¹⁻⁶. Rapid analysis is essential in pathogen detection, especially for diagnosis of pathogen infection and controlling the spread of infectious diseases^{3, 5, 7, 8}. Conventional culture and colony counting method uses specific microbiologic media to isolate and enumerate a pathogen species. This method is sensitive and accurate, but it is also time consuming and requires complex procedures¹. Nucleic acid-based methods such as polymerase chain reaction (PCR) assay have been used in pathogen detection because of their high sensitivity^{7, 9, 10}. However, they either require long reaction time or multi-step sample preparation procedures including cell lysis and 5 - 24 hours long enrichment steps¹¹. Hence it is challenging for rapid, onsite pathogen detection. A conventional immunoassay such as an enzyme-linked immunosorbent assay (ELISA)^{5, 12, 13} is highly specific and applicable to pathogen detection; however, it also requires long assay time. Furthermore, both PCR and ELISA methods require bulky, expensive instruments and highly trained personnel¹⁴. Recently, lab-on-a-chip immunosensors have attracted attentions for bacterial pathogen detection because of their capability of direct cell measurements without needs for cell lysis or pre-enrichment while having high specificity^{2, 11, 15, 16}. An immunosensor chip transduces the specific binding between receptors on cell surface and antibodies immobilised on a solid surface to an electrical or optical signal^{2, 17-19}. While the surface immobilisation of antibody is crucial for sensitivity of an immunosensor³, it is a great challenge to make the surface modification by antibodies in microchannels, and maintain functionality of the surface modification for a long time, due to the

instability of antibodies²⁰. Regenerating the surface modification of a microchannel is also a challenge to reuse the sensor^{21, 22}.

To overcome the above limitations, we report a device for pathogen detection using a simple surface functionalization method by attaching antibody-functionalized microparticles (Ab-MPs) to the sensing surface via an applied magnetic field, requiring no chemical modification of the sensor surface. The sensing surface can be functionalized quickly before each test, and can also be regenerated by removing the magnetic field and washing away the magnetic microparticles. Coupled with a two-stage resistive pulse sensor, this device can accurately detect and count the pathogen cells in a mixture. Using *S. cerevisiae* as a model pathogen cell, we proved that this device is able to quantitatively detect the *S. cerevisiae* from a mixed population with *Chlorella*, which is used as model non-target cells.

Sensing Principle and Design Concept

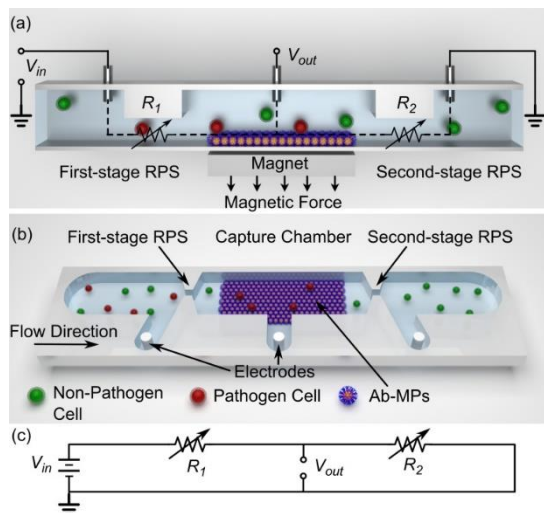


Fig. 1. Schematic of the two-stage resistive pulse sensor (RPS) for pathogen cell detection. (a) schematic cross-section view showing the capture chamber is coated with a thin layer of Ab-MPs to catch the pathogen cells. The two-stage RPS are modelled as two variable resistors connected in series, (b) 3-D view of the two-stage RPS consists of a pair of RPSs, a capture chamber and three electrodes, and (c) equivalent circuit of the two-stage RPS.

Figure 1 illustrates mechanism of the pathogen detection. The detection consists of four major steps: firstly, antibody binds to dynabeads protein G through Fc-region to form antibody functionalized microparticles (Ab-MPs). Secondly, Ab-MPs are then loaded to the device and form a thin layer of Ab-MPs on the bottom of the capture chamber owing to attraction forces by an external magnet, as shown in Fig. 1 (a). Thirdly, cells are loaded to the device. Because of the specific binding between the receptors on pathogen surface and Ab-MPs surface, pathogen cells are captured by the Ab-MPs layer in the capture chamber, while non-target cells travel to the 2nd stage resistive pulse sensor (RPS), as shown in Fig 1. Finally, the two-stage resistive pulse sensor is used to count and size the cells passing through them. The 1st stage RPS counts all cells in a sample, while the 2nd stage RPS counts only the non-target cells. The count difference between the two RPSs represents the population of pathogen cells in the tested sample. Unlike the conventional micro immunoassay, this approach eliminates the need to chemically modify the surface of microchannels, which is typically difficult and time consuming on a chip, and has a limited shelf life²³. The Ab-MPs layer attached on the capture chamber is easy to be regenerated by simply removing the magnetic field, washing away the old Ab-MPs and refilling fresh Ab- MPs, making this device is easy to recover for next use.

Device fabrication and testing procedure

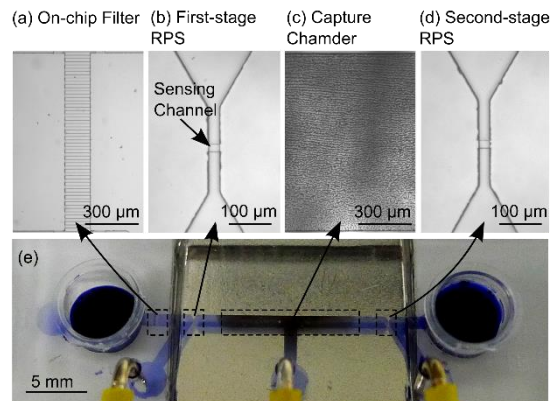


Fig. 2. Images (a) On-chip filter, (b) 1st stage RPS with a sensing channel of 30 μm × 20 μm × 20 μm (Length × Width × Height), (c) the surface of the capture chamber functionalized with layers of Ab-functionalized MPs by an external magnet, (d) 2nd stage RPS with an identical sensing channel to 1st first stage RPS, (e) the two-stage RPS device consists of inlet and outlet reservoirs, two RPSs, a capture chamber with Ab-functionalized MP coating, and three Ag/AgCl electrodes.

The resistive pulse sensor was fabricated using standard soft lithography method. It consists of 1) two resistive pulse sensing channels with a width of 20 μm, and length of 30 μm to detect cell transits; 2) a capture chamber with a width of 1 mm and a length of 15 mm to capture pathogen cells, 3) three Ag/AgCl electrodes to detect the resistive pulses caused by passages of cells through 1st RPS and 2nd RPS, and 4) a filter structure with pore width of 20 μm. A two layer SU8 mold, consisting patterns for the sensing channel and the filter with a thickness of 20 μm and patterns for the capture chamber and the reservoirs with a thickness of 40 μm, was created by a two-step photolithography process²³. The microchannels, capture chamber and reservoirs were then formed by pouring Polydimethylsiloxane (PDMS) onto the two-layer SU8 mold followed by degassing and curing. This two-layer structure offers a higher sensitivity of the sensing channel without increasing the flow resistance of reservoirs. Next, PDMS microchannel was bonded onto a glass substrate after an oxygen plasma treatment (200 mTorr, 50 W, 50 s). Ag/AgCl electrodes were inserted on each side of the sensing channels to finish the fabrication of the two-stage RPS.

Next, 100 μL of Ab-MPs were loaded into the inlet reservoir and driven through the capture chamber by pressure difference between inlet and outlet reservoir, at a flow rate of approximately 200 μL/hr. An external magnet (19 mm × 19mm × 19mm, NdFeB, Grade N52, K&J Magnetics, Inc.) was used to capture the Ab-MPs in order to form an Ab-MP coating layer on the bottom of the capture chamber. 50 μL of Ab-MPs with a concentration of 7.2×10^4 counts/μL was loaded to the device. After the Ab-MP coating was formed, non-captured MPs were removed from the inlet reservoir. The device was washed by PBS buffer. Approximately 3.6×10^6 counts of Ab-MPs were loaded to the capture chamber, and were estimated to form ~2 layers of Ab-MPs (The estimated thickness of Ab-MPs coating is 5.3 μm). For each test, 100 μL of sample containing pathogen cells were loaded into the inlet reservoir at a flow rate of 20 μL/hr. To provide the pressure difference between inlet and outlet reservoir, the device was placed vertically and the sample were driven through the device by gravity. The flow rate was calculated using the volume difference in the inlet reservoir before and after each test, divided by the time duration of each test. Resistive pulses from the two resistive pulse sensors were recorded by a data

acquisition card (NI USB-6251, National Instruments) at a sampling rate of 500 kHz²³.

Sample preparation

Saccharomyces cerevisiae (ATCC, Manassas, VA USA) and *Chlorella* (Carolina Biological Supply Company, Burlington, NC USA) were used as model pathogen cells and non-target pathogen cells, respectively, to prove the concept of the two-stage resistive pulse sensor. *S. cerevisiae* was cultured in the medium (3 g of yeast extract, 3 g of malt extract, 5 g of trypton, 10 g of glucose in 1 liter DI water) for 18 hours, then collected by centrifuging at 2200 rpm, followed by being washed twice with phosphate buffer saline (PBS, pH 7.4, Sigma-Aldrich, USA) containing 0.1% bovine serum albumin (BSA, Sigma-Aldrich, USA). Next, the collected cells were resuspended at preferred concentrations ranging from 1.0 cells/ μL to 1.8×10^4 cells/ μL .

Chlorella was cultured by transferring 10 mL of a stock culture directly from the vendor into 200 mL of Alga-Gro fresh water medium (Carolina Biological Supply Company). The new culture was placed under cool-white fluorescent lights for 7 to 10 days to allow the algae to grow. Then *Chlorella* was collected by centrifuging at 5000 rpm, washed twice with PBS containing 0.1% BSA and resuspended at a concentration of 1.0×10^3 cells/ μL .

To prepare Ab-MPs, firstly, dynabeads protein G with a diameter of 2.80 μm (10 mg/mL, Life Technologies, USA) was diluted 1/50 in PBS with 0.1% BSA. The polyclonal Ab to *S. cerevisiae* (Ab1, 1 mg/ml, Bio-Rad, USA) was diluted 1/25 in PBS with 0.1% BSA. Next, 50 μL of diluted MP solution was mixed with 50 μL diluted Ab solution for 30 min on a thermal mixer at a speed of 650 rpm at room temperature. The MP solution was then placed on a magnet to separate MPs from the solution, and the supernatant containing unconjugated Abs was removed. The separation and removal processes were repeated for three times to remove all unconjugated Abs. Next, Ab-MPs were resuspended in PBS with 0.1% BSA at a concentration of 0.2 mg/mL. Additionally, the rabbit anti-mouse antibody (Ab2, 1 mg/mL, Life Technologies, USA) was also conjugated with MPs using the same procedure, which was used for control experiments.

Results and Discussions

Yeast is a group of important microorganisms for many biology studies²⁴. Some species of yeast, for example, *Candida albicans*, can cause infections in humans^{25, 26}. *S. cerevisiae* is well-known in bakery or brewing industry; however, it is also reported as an unusual cause of life-threatening infection in humans²⁷⁻²⁹. In our study, *S. cerevisiae* is used as a model cell to prove the concept of the pathogen detection mechanism shown in Fig. 1. *Chlorella* was used as the control cell, whose size is very close to that of *S. cerevisiae*, to prove the device's capability to detect target cells from similar-sized reference cells. In our study, the concentration of *S. cerevisiae* was varied from 1.0 to 1.8×10^4 cells/ μL , while the *Chlorella* concentration was kept constantly at 1.0×10^3 cells/ μL . The cell concentrations were measured using an Accusizer 780 particle sizer (Particle Sizing Systems, Port Richey, FL USA) before each test. We also measured the sizes of both cells using a light microscope. The size ranges of *S. cerevisiae* and *Chlorella* were from 3.2 to 7.4 μm and from 3.4 to 8.4 μm . The on-chip filter was able to block any debris larger than 20 μm .

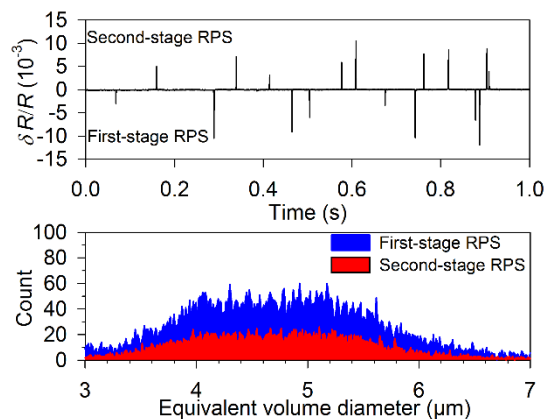


Fig. 3. (a) Relative resistive pulses caused by cell transits. Negative and positive pulses represent cell passages through 1st stage RPS and 2nd stage RPS, respectively; (b) counts and size distribution measured from 1st stage RPS (before the capture chamber) and 2nd stage RPS (after the capture chamber). During this test, 13.74×10^3 cells entered the capture chamber, while 7.37×10^3 cells exited the chamber. Both *S. cerevisiae* and *Chlorella* had a concentration of 1.0×10^3 cells/ μL .

Fig. 3 (a) shows typical relative voltage pulses generated by the two RPSs when 7 μL mixed sample of *S. cerevisiae* and *Chlorella* was tested. Both *S. cerevisiae* and *Chlorella* had a concentration of 1.0×10^3 cells/ μL . As shown in Fig. 1 (c), the two-stage RPS is modelled as two variable resistors connected in series. The output voltage, v_{out} , was measured at the central electrode. A cell passing through the sensing channel of 1st stage RPS increases the resistance of the channel, causing a decrease in v_{out} , (negative voltage pulse). Similarly, a cell passing through 2nd stage RPS also causes an increase in resistance, but generates a positive voltage pulse of v_{out} . Hence each positive pulse represents a cell transit through the 2nd stage RPS, and the negative pulse represents a cell transit through 1st stage RPS. The cell volume is proportional to the magnitude of the resistive pulses ($\delta R/R$)^{30, 31}.

$$\delta R/R = (d^3/LD^2) \cdot \left[(D^2/2L^2) + 1/\sqrt{1+(D/L)^2} \right] \cdot F(d^3/D^3) \quad (1)$$

where R is the resistance of a sensing channel, d is the equivalent volume diameter of a particle, D and L are the characteristic diameter and the length of the rectangular sensing channel, F is the correction factor. In our design, D was calculated to be 22.6 μm by $D = (4 \cdot A/\pi)^{1/2}$, where A is the cross-sectional area of the sensing channel, F was taken to be 1.0³². After the 20 μL sample were tested in the device, each cell size was back calculated from its resistive pulse ($\delta R/R$), which was derived from the equivalent circuit (see Fig. 1(c)), using equation 1. The cell size distributions and counts measured by 1st and 2nd RPSs are shown in Fig. 3 (b). Fig. 3(b) shows the following: 1) a total of 13.74×10^4 cells passed through the 1st RPS and entered the capture chamber, while 7.37×10^3 *Chlorella* cells exited the chamber, implying 6.73×10^3 *S. cerevisiae* were captured by the capture chamber. The total counts for *S. cerevisiae* and *Chlorella* are in good agreement with the actual numbers calculated from their concentration (*S. cerevisiae*: 7×10^3 , *Chlorella*: 7×10^3 and total counts: 14×10^3). The measured sizes of *S. Cerevisiae* and *Chlorella* also match the microscopic measurement well.

It is worthwhile mentioning here that the pathogen cell measurement relies on an assumption that all pathogen cells are captured by the Ab-MP layer while all non-target cells are not captured by the layer. Accurate detection requires the reduction of the cell counts between 1st and 2nd stage RPS are caused by the specific capture of pathogen (*S. cerevisiae*) by the Ab-MP layer. However, in actual measurements, the reduction could also be caused by the non-specific attachment of non-target cells (*Chlorella*). To prove the dominance of specific capture, experiments were conducted to evaluate the capture efficiency of specific and non-specific attachment by the Ab-MP layer using two types of Ab-functionalized MPs: 1) anti-*S. cerevisiae* Ab-functionalized MPs (Ab1-MPs) coated on the capture chamber to evaluate the specific capture of *S. cerevisiae*, and non-specific capture of *Chlorella*, and 2) rabbit anti-mouse Ab-MPs (Ab2-MPs) coated on the capture chamber to evaluate the non-specific capture of *S. cerevisiae* and *Chlorella*, respectively. The cell concentration and flow rate were set to be 1.0×10^3 cells/ μL and 20 $\mu\text{L}/\text{hr}$ for both experiments. For each test, only one type of cells was used. The capture efficiency is defined as the ratio of the count of cells captured in the chamber over the count of cell entering the capture chamber; both counts were obtained from the counts of two RPSs. Each test was repeated five times. The measurement results on capture efficiency of *S. cerevisiae* and *Chlorella* under two chamber surface conditions are shown in Figure. 4.

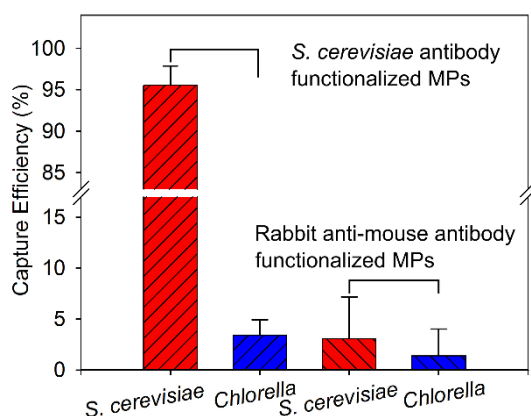


Fig. 4. Measured capture efficiency of *S. cerevisiae* and *Chlorella* with anti-*S. cerevisiae* Ab-functionalized MPs and rabbit anti-mouse-MPs.

As shown in Fig. 4, with Ab1-MPs, the capture efficiency for *S. cerevisiae* and *Chlorella* were $95.5 \pm 2.3\%$ (specific capture efficiency) and $3.4 \pm 1.5\%$ (nonspecific capture efficiency). With the Ab2-MPs, the nonspecific capture efficiencies for *S. cerevisiae* and *Chlorella* were $3.1 \pm 4.1\%$, and $1.4 \pm 2.6\%$. Although the capture efficiency is highly dependent on the affinity of the antibody, the capture ligand and the contact time of the cell and the surface, the 94.8% capture efficiency is very high in this initial evaluation. The non-specific attachment (<5%) is low, and is comparable with the non-specific attachment reported by other studies^{2, 17}. With the high specific capture efficiency and the low nonspecific capture efficiency, the proposed device is expected to differentiate and count pathogen cells accurately from a mixture with small errors. To confirm the reproducibility, we repeated the capture efficiency tests on two additional devices with the same design. Using the same Ab1-MPs and the same procedure, the specific capture efficiency of *S. cerevisiae* was 94.2% and 96.1%, and nonspecific capture

efficiency of *Chlorella* was 3.4% and 1.4% (See ESI, Figure S2), which are close to those of the device shown in Fig. 4.

Note that the non-specific attachment can be further reduced by optimizing the shear stress³⁰. A recent study showed that shear stress ranging from 1.0 to 3.0 dyn/cm² was an optimal shear stress in CD4+ T cell capture¹⁷. The shear stress was estimated using following equation^{18, 33}.

$$\tau_w = 6\mu Q/(h^2w) \quad (2)$$

where τ_w is the shear stress at the walls of a rectangular channel, μ is the dynamic viscosity of the fluid, Q is the flow rate, w is the width of microfluidics channel and h is the height of the microfluidics channel. In our test, the dynamic viscosity of PBS buffer was 1×10^{-3} Pa·s³⁴, and the flow rate was 20 $\mu\text{L}/\text{hr}$. Hence the shear stress is estimated to be 0.21 dyn/cm². We believe an increased flow rate may further reduce the non-specific attachment. However, a large flow rate may wash away the Ab-MPs later; a strong magnetic field may be needed for a larger flow rate. In addition, the non-specific attachment can also be reduced by (1) increasing the antibody density on MP surface and the Ab-MP coverage on the sensing surfaces, and 2) using antifouling materials to modified MP and sensor surfaces.

To evaluate the concentration measurement accuracy, pure *S. cerevisiae* with different concentrations ranging from 1.0 to 1.8×10^4 cells/ μL were tested by both the two-stage RPS with Ab1-MPs coating on the capture chamber and the Accusizer. In the two-stage RPS device, the capture chamber is expected to capture most of the cells.

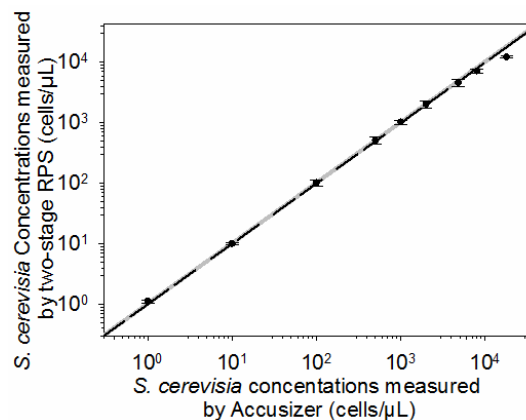


Fig. 5. The comparison of *S. cerevisiae* concentration measured by a two-stage RPS and Accusizer. The concentration was varied from 1.0 to 1.8×10^4 cells/ μL . The black dash line represents $y = x$ line. The shaded region represents the measurement uncertainty of the Accusizer ($\pm 10\%$, from the manual of Accusizer 780 Particle Sizing System). The measured concentration was fitted with $y = x$, the R^2 is great than 98%.

Fig. 5 shows the measurement results, indicating the concentration measured by the two-stage RPS (black circles) are in good agreement with that measured by the Accusizer. From the responses of the 1st stage RPS and the 2nd stage RPS, the capture efficiency was calculated to range from 93.5 to 96.0%, which is high and comparable to the result report by other studies^{17, 35}. The capture efficiency can be further increased by 1) using a longer capture

chamber to promote interactions between cells and Ab-MPs, and 2) using antibody or aptamer with higher binding affinity^{36, 37}. To determine the detection limit, we measured the particle concentration of a blank PBS buffer. The test was repeated 5 times. The measured particle concentration was 0.3 ± 0.1 counts/ μL . The limit of detection (f_{LOD}) is given by³⁸:

$$f_{LOD} = f_0 + 3 \times \sigma_0 \quad (3)$$

where f_0 is the particle concentration of the PBS buffer, σ_0 is the standard deviation. With $f_0 = 0.3$, $\sigma_0 = 0.1$, f_{LOD} is 0.6 cells/ μL from equation 3. A t-test also showed the difference between PBS buffer (0.3 ± 0.1 cells/ μL , $N=5$) and 1.0 cells/ μL sample (1.1 ± 0.1 cells/ μL , $N=5$) was statistically significant (P -value < 0.0001). Hence the resolution of the current method was estimated to be up to 1.0 cells/ μL . We also experimentally determined the upper limit of detection was 8.0×10^3 cells/ μL with the current detection algorithm. At higher cell concentrations, the chance that two cells transit through a sensing channel at same time increased, which will lead to a larger measurement error. The experiment results show a large error ($31.9\% \pm 3.3\%$, as show in Fig. 5) at the concentration of 1.8×10^4 cells/ μL . It is worth to mention that because a two-cell passage generates a complex pulse, an advanced pattern recognition algorithm can be used to differentiate a single cell passage from a two-cell passage³⁹; the upper detection limit can be increased. The detection range was from 0.6 to 8.0×10^3 cells/ μL . For a diluted sample with lower cell concentrations (i.e., 1.0 cells/ μL), a relatively large volume of samples needs to be analyzed to ensure detection accuracy, leading to longer detection time. However, several methods, such as centrifugation or a multichannel resistive pulse sensor⁴⁰ can be used to reduce the assay time. In the detection range from 1.0 to 8.0×10^3 cells/ μL . The measurement error is between 1.4 to 11.2%. The relationship between *S. cerevisiae* concentrations measured by the two-stage RPS and Accusizer was fitted with the reference line $y = x$ in the concentration range from 1.0 to 8.0×10^3 cells/ μL , and the coefficient of determination, R^2 , was greater than 0.98. A t-test was conducted on the concentration measurements. The p-values for all measurements were less than 0.001 at 95% confidence interval, showing each measured concentration can be significantly distinguished from other concentrations. Another factor, which may affect the measurement accuracy at a higher concentration at a higher concentration, is the increased chance of two cells transit through two sensing channels at the same time, that may cause increase of both R_1 and R_2 (see Fig. 1) and lead to incorrect count and incorrect concentration measurement. This issue can be overcome by taking two independent measurements of the two RPSs, using two pairs of electrodes.

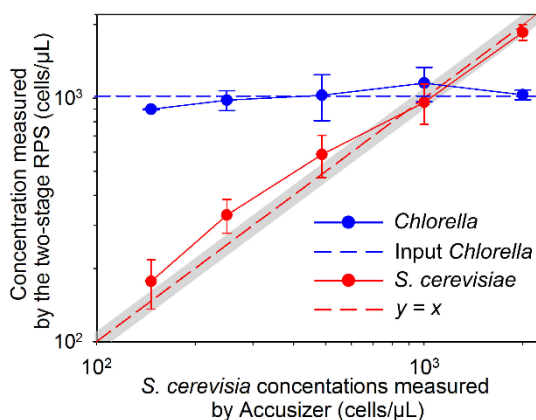


Fig. 6. Measured *S. cerevisiae* in a mixed population of *S. cerevisiae* and *Chlorella*. The concentration of *S. cerevisiae* was varied from 1.5×10^2 to 2.0×10^3 cells/ μL . The concentration of *Chlorella* was kept constant (1.0×10^3 cells/ μL). The shade region represents the measurement uncertainty of the Accusizer ($\pm 10\%$, from the manual of Accusizer 780 Particle Sizing System).

Next, we demonstrated *S. cerevisiae* detection in a mixed population of *S. cerevisiae* and *Chlorella*. The concentration of *S. cerevisiae* was varied from 1.5×10^2 to 2.0×10^3 cells/ μL , while the concentration of *Chlorella* was kept constant, 1019 cells/ μL . The measured *S. cerevisiae* concentration vs the input concentration was plotted in Fig. 6. For comparison, $y = x$ line and $y = 1 \times 10^3$ cells/ μL line were also plotted. The *Chlorella* concentration measured by our device and by Accusizer at all *S. cerevisiae* concentrations was 1018 ± 92 cells/ μL and 1019 ± 69 cells/ μL , which agreed with each other very well, indicating the nonspecific capture efficiency is low. For *S. cerevisiae* measurement, the measured concentrations by the two-stage RPS device are accurate when the *S. cerevisiae/Chlorella* ratio (target cell to non-target cell ratio) is high (from 1.0 to 2.0). Compared to the Accusizer measurements, the measurement error ranged from 4 to 7%, which is well within the measurement uncertainty of the Accusizer. The best accuracy was achieved at a *S. cerevisiae/Chlorella* ratio equalling to one. We also expect a low measurement error when *S. cerevisiae* concentration is greater than 2.0×10^3 cells/ μL , because the amount of nonspecific captured *Chlorella* cells is much small compared to the large amount of *S. cerevisiae* cells. However, at lower *S. cerevisiae/Chlorella* ratios (0.1 to 0.5), the measurement error became higher, ranging from 20% to 32%, which was 10% to 22% higher than the measurement uncertainty of the Accusizer. Note that the detection accuracy is affected by the ratio of target/non-target cells due to the nonspecific attachment of non-target cells. At low target cell/non-target cell ratios, the detection accuracy decreases because even a small amount of nonspecific attachment causes large error in detection of target cells whose concentration is low, which is an universal challenge for all cell immunoassays. For example, previous study⁴¹ demonstrated that 58.2% of target *L. monocytogenes* was captured when it is mixed with non-target *S. Enteritidis* at 1:1 ratio. In our experiment, the relative error on *S. cerevisiae* concentration measurement was 4% when the *S. cerevisiae/Chlorella* ratio is 1.0, indicating our method has much higher capture efficiency and higher accuracy. The accuracy can be further improved by using a capture ligand with a higher affinity, a higher flow rate and/or antifouling surfaces^{42, 43}. We conducted statistical analysis on the concentration measurement. The p-values for all measurements shown in Fig. 6 were less than 0.005 at 95% confidence interval, showing each measured concentration can be significantly distinguished from other concentrations.

The advantages of the presented pathogen cell detection method are manifold. First, it eliminates the need for on-chip surface modification, which is typically difficult and time consuming for microchannels; secondly, the sensing surface can be functionalized right before each test using freshly-made Ab-MPs. This greatly improves the device reliability because antibodies has a limited shelf life due to irreversible denaturation²⁰. Thirdly, the Ab-MP based capture surface enables high capture efficiencies due to increased surface roughness. Fourthly, the sensing surface functionalization can be regenerated quickly by removing the magnetic field and washing away the magnetic beads for next use. With these advantages, this device can be potentially used for a range of applications in addition to microorganism identification. For

example, it can potentially be used for HIV diagnosis, where CD4/CD8 T lymphocyte ratio less than one is a possible HIV indicator⁴⁴. The device can also be extended to detect multiple types of pathogen cells in a single test by using multiple capture chambers in series, with each chamber coated with one specific Ab-MPs layer.

Conclusions

We reported a microfluidic immunosensor for pathogen measurement without a need for on-chip chemical modification of microchannels. Antibody-functionalized microparticles were used to functionalize the capture chamber surface and a two-stage resistive pulse sensor was used to detect and count pathogen cells. We demonstrated that this device is capable to achieve the high specific capture efficiency greater than 94.8%, and the non-specific capture efficiency as low as 3.4%. We also demonstrated that the device can measure the *S. cerevisiae*/Chlorella ratio ranging from 1.0 to 2.0, the measurement error ranged from 4 to 7%, while the errors were 20 to 32%, for the ratio was 0.1 to 0.5. Without using surface modification process, this device enables a fast and cost-effective pathogen detection and microorganism identification.

Acknowledgements

This work is supported by the National Science Foundation under award #1200032.

Notes and references

^aDepartment of Mechanical Engineering, University of Akron, OH USA
Email: jzhe@uakron.edu; Fax:+1(330) 972 6027; Tel: +1 (330) 972 7737.

^bDepartment of Chemical and Biomolecular Engineering, University of Akron, OH USA. Email: gc@uakron.edu; Fax:+1(330) 972 5856; Tel: +1 (330) 972 8680.

‡Equal contribution.

- B. Swaminathan and P. Feng, *Annual Reviews in Microbiology*, 1994, **48**, 401-426.
- D. A. Boehm, P. A. Gottlieb and S. Z. Hua, *Sensors and Actuators B: Chemical*, 2007, **126**, 508-514.
- O. Lazcka, F. J. Del Campo and F. X. Munoz, *Biosensors and Bioelectronics*, 2007, **22**, 1205-1217.
- V. Velusamy, K. Arshak, O. Korostynska, K. Oliwa and C. Adley, *Biotechnology advances*, 2010, **28**, 232-254.
- J. Mairhofer, K. Roppert and P. Ertl, *Sensors*, 2009, **9**, 4804-4823.
- A. Singh, S. Poshtiban and S. Evoy, *Sensors*, 2013, **13**, 1763-1786.
- P. Belgrader, W. Benett, D. Hadley, G. Long, R. Mariella, F. Milanovich, S. Nasarabadi, W. Nelson, J. Richards and P. Stratton, *Clinical chemistry*, 1998, **44**, 2191-2194.
- P. Mandal, A. Biswas, K. Choi and U. Pal, *American Journal Of Food Technology*, 2011, **6**, 87-102.
- S. Saglani, K. Harris, C. Wallis and J. Hartley, *Archives of disease in childhood*, 2005, **90**, 70-73.
- B. Malorny, P. T. Tassios, P. Rådström, N. Cook, M. Wagner and J. Hoorfar, *International journal of food microbiology*, 2003, **83**, 39-48.
- A. M. Foudeh, T. F. Didar, T. Veres and M. Tabrizian, *Lab on a Chip*, 2012, **12**, 3249-3266.
- R. Haque, K. Kress, S. Wood, T. F. Jackson, D. Lyster, T. Wilkins and W. A. Petri, *Journal of Infectious Diseases*, 1993, **167**, 247-249.
- W. Puppe, J. Weigl, G. Aron, B. Gröndahl, H.-J. Schmitt, H. Niesters and J. Groen, *Journal of clinical virology*, 2004, **30**, 165-174.
- J. C. Jokerst, J. A. Adkins, B. Bisha, M. M. Mentele, L. D. Goodridge and C. S. Henry, *Analytical chemistry*, 2012, **84**, 2900-2907.
- D. Figeys and D. Pinto, *Analytical Chemistry*, 2000, **72**, 330 A-335 A.
- J.-Y. Yoon and B. Kim, *Sensors*, 2012, **12**, 10713-10741.
- X. Cheng, D. Irimia, M. Dixon, K. Sekine, U. Demirci, L. Zamir, R. G. Tompkins, W. Rodriguez and M. Toner, *Lab on a Chip*, 2007, **7**, 170-178.
- N. N. Watkins, S. Sridhar, X. Cheng, G. D. Chen, M. Toner, W. Rodriguez and R. Bashir, *Lab on a Chip*, 2011, **11**, 1437-1447.
- A. Carbonaro, S. K. Mohanty, H. Huang, L. A. Godley and L. L. Sohn, *Lab on a Chip*, 2008, **8**, 1478-1485.
- S. D. Jayasena, *Clinical chemistry*, 1999, **45**, 1628-1650.
- P. D. Skottrup, M. Nicolaisen and A. F. Justesen, *Biosensors and Bioelectronics*, 2008, **24**, 339-348.
- F. C. Dudak and İ. H. Boyacı, *Biotechnology journal*, 2009, **4**, 1003-1011.
- Y. Han, H. Wu, F. Liu, G. Cheng and J. Zhe, *Analytical chemistry*, 2014, **86**, 9717-9722.
- D. Botstein, S. A. Chervitz and J. M. Cherry, *Science (New York, NY)*, 1997, **277**, 1259.
- M. McCullough, B. Ross and P. Reade, *International journal of oral and maxillofacial surgery*, 1996, **25**, 136-144.
- A. H. Groll, N. Giri, V. Petraitis, R. Petraitiene, M. Candelario, J. S. Bacher, S. C. Piscitelli and T. J. Walsh, *Journal of Infectious Diseases*, 2000, **182**, 274-282.
- J. N. Aucott, J. Fayen, H. Grossnicklas, A. Morrissey, M. M. Lederman and R. A. Salata, *Review of Infectious Diseases*, 1990, **12**, 406-411.
- P. Muñoz, E. Bouza, M. Cuenca-Estrella, J. M. Eiros, M. J. Pérez, M. Sánchez-Somolinos, C. Rincón, J. Hortal and T. Peláez, *Clinical Infectious Diseases*, 2005, **40**, 1625-1634.
- R. H. Eng, R. Drehmel, S. M. Smith and E. J. Goldstein, *Medical Mycology*, 1984, **22**, 403-407.
- A. V. Jagtiani, J. Carletta and J. Zhe, *Journal of Micromechanics and Microengineering*, 2011, **21**, 045036.
- A. Carbonaro and L. Sohn, *Lab on a Chip*, 2005, **5**, 1155-1160.
- R. DeBlois and C. Bean, *Review of Scientific Instruments*, 1970, **41**, 909-916.
- S. Usami, H.-H. Chen, Y. Zhao, S. Chien and R. Skalak, *Annals of biomedical engineering*, 1993, **21**, 77-83.
- F. Momen-Heravi, L. Balaj, S. Alian, A. J. Trachtenberg, F. H. Hochberg, J. Skog and W. P. Kuo, *Frontiers in physiology*, 2012, **3**, 162.
- J. G. Kralj, C. Arya, A. Tona, T. P. Forbes, M. S. Munson, L. Sorbara, S. Srivastava and S. P. Forry, *Lab on a Chip*, 2012, **12**, 4972-4975.

Journal Name

36. Y. A. Yeung and K. D. Wittrup, *Biotechnology progress*, 2002, **18**, 212-220.
37. J. Zhang, W. Sheng and Z. H. Fan, *Chemical Communications*, 2014, **50**, 6722-6725.
38. G. L. Long and J. D. Wineford, *Analytical chemistry*, 1983, **55**, 712-724.
39. E. J. W. Wynn and M. J. Hounslow, *Powder Technology*, 1997, **93**, 163-175.
40. J. Zhe, A. Jagtiani, P. Dutta, J. Hu, and J. Carletta, *J. Micromechanics Microengineering*, 2007, **17**, 304-313.
41. A. Foddai, C. T. Elliott and I. R. Grant, *Applied and environmental microbiology*, 2010, **76**, 7550-7558.
42. B. Cao, L. Li, H. Wu, Q. Tang, B. Sun, H. Dong, J. Zhe and G. Cheng, *Chem. Commun.*, 2014, **50**, 3234-3237.
43. B. Cao, Q. Tang, L. Li, J. Humble, H. Wu, L. Liu and G. Cheng, *Advanced healthcare materials*, 2013, **2**, 1096-1102.
44. J. M. G. Taylor, J. L. Fahey, R. Detels, and J. V. Giorgi, *Journal of Acquired Immune Deficiency Syndromes*, 1989, **2**, 114-124.